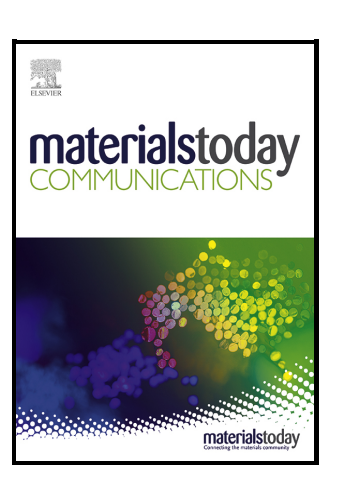
Journal Pre-proof

Fish skin gelatin nanofibrous scaffolds spun using alternating field electrospinning and *in-vitro* tested with tdTomato mice fibroblasts

Amanda Kennell, Mark MacEwen, Micah Armstrong, Teodora Nicola, Brian Halloran, Namasivayam Ambalavanan, Andrei Stanishevsky



PII: S2352-4928(22)00286-0

DOI: https://doi.org/10.1016/j.mtcomm.2022.103417

Reference: MTCOMM103417

To appear in: Materials Today Communications

Received date: 2 July 2021 Revised date: 5 February 2022 Accepted date: 18 March 2022

Please cite this article as: Amanda Kennell, Mark MacEwen, Micah Armstrong, Teodora Nicola, Brian Halloran, Namasivayam Ambalavanan and Andrei Stanishevsky, Fish skin gelatin nanofibrous scaffolds spun using alternating field electrospinning and *in-vitro* tested with tdTomato mice fibroblasts, *Materials Today*Communications, (2021)

doi:https://doi.org/10.1016/j.mtcomm.2022.103417

This is a PDF file of an article that has undergone enhancements after acceptance, such as the addition of a cover page and metadata, and formatting for readability, but it is not yet the definitive version of record. This version will undergo additional copyediting, typesetting and review before it is published in its final form, but we are providing this version to give early visibility of the article. Please note that, during the production process, errors may be discovered which could affect the content, and all legal disclaimers that apply to the journal pertain.

© 2021 Published by Elsevier.

Fish skin gelatin nanofibrous scaffolds spun using alternating field electrospinning and *invitro* tested with tdTomato mice fibroblasts.

Amanda Kennell^{a*}, Mark MacEwen^b, Micah Armstrong^c, Teodora Nicola^b, Brian Halloran^b, Namasivayam Ambalavanan^b, Andrei Stanishevsky^a

^a Department of Physics, University of Alabama at Birmingham, Birmingham, Al 35294, USA

^b Department of Pediatrics, University of Alabama at Birmingham, Birmingham, AL 35249

^c Department of Materials Science and Engineering, University of Alabama in Birmingham, Birmingham, AL 35233

*corresponding author email: akennell@uab.edu, postal address: University of Alabama at Birmingham, 1300 University Boulevard, Birmingham, AL 35294-1170, USA

Abstract

There is a strong need for the mass production of biomaterials, as tissue engineering shows promising results in transplant surgeries. This research presents preliminary results on a "green" method of constructing a biomaterial that is bioactive, biocompatible, and suitable for scale-up manufacturing. This was done by producing nanofibrous fish skin gelatin (FSG) scaffolds from an aqueous precursor using a high throughput alternating field electrospinning (AFES) method. The nanofibrous FSG material was produced at 12.6 g/h and could include carboxymethyl cellulose (cmCEL) as an additive to improve mechanical properties. To keep the process environmentally safer, thermal crosslinking was used to control the scaffolds biodegradation rate

and maintain a uniform fiber diameter distribution of 175±19 nm. Scanning electron microscopy indicated similarities between the scaffold and the extracellular matrix (ECM). The scaffold's biocompatibility was verified with *in-vitro* testing utilizing naturally fluorescent tdTomato mice fibroblasts. The cmCEL loaded FSG scaffold demonstrated 11.5% higher cell proliferation after 72 h compared to the pure FSG scaffold. Also, the cmCEL loaded scaffolds had more uniform cell distribution (235±80 cells/mm²) then the FSG scaffold (251±179 cells/mm²). The results demonstrate a uniform nanofibrous ECM with favorable cell response can be reproducibly made with a high productivity rate through AFES.

Key Words: Alternating Field Electrospinning, Nanofibers, Fish Skin Gelatin, tdTomato Mice Fibroblasts, Extracellular matrix

1. Introduction

Tissue engineering (TE) with nanofibrous materials shows promising results in transplant surgeries where there is a strong need for a sustainable production of natural biomaterials. Tissue repair starts by making an extracellular matrix (ECM). Developing a structure that mimics the ECM (ECM mimic) has had a limited rate of success [1]. Also, the issues for safely developing this backbone, the ECM mimic, have not yet been overcome. Electrospun natural biopolymers are attractive for developing this ECM mimic but their production is very limited. This study proposes a "green" electrospinning method to overcome some current limitations in TE to make a viable, sustainably, and manufacturable ECM mimic.

The body's natural response to heal from a trauma is laying a collagen web called the ECM. This ECM web consists mainly of collagen with elastin, fibrin, and other macromolecules [2]. In order to skip this first step in tissue repair, an ECM mimic can be made from an electrospun nanofibrous scaffold. As collagen makes up the largest portion (30%) of the ECM [2,3] many current scaffolds are made from collagen [4]. However, electrospinning a collagen scaffold is difficult, as collagen needs harsh chemicals to become soluble. Additionally, collagen has been suspected to transfer diseases to its host through prions [5,6]. Collagen also needs additives such as fibronectin to further promote cell proliferation and control the ECM's degradation rate [7]. Another necessary additive is elastin (also natural to the body's ECM) which makes the collagen based ECM malleable enough [8]. Fibronectin and elastin are expensive and time consuming to process and electrospin, which further complicates the collagen ECM's process.

Ideal biomaterials must demonstrate an optimal level of biocompatibility, biodegradability, and bioactivity to induce a favorable response from the body's immune system. Even though collagen is natural it has deficiencies, as mentioned previously, in electrospun productivity rate and unfavorable use of harsh solvents. Gelatin, a derivative of collagen, has more desirable properties [9,10] for an ECM mimic. Gelatin is easier to electrospin then collagen, it has been shown to not transfer diseases to its host [6], and it is more environmentally friendly as it can be fully soluble in a pure aqueous solution [11]. On its own gelatin is naturally elastic [10] indicating that there is no need for additives to improve a gelatin ECM's elasticity. Gelatin also stimulates cell proliferation [11,12], is biodegradable [11], and has a controllable biodegradation rate through crosslinking. However, the mechanical properties of gelatin alone are not fully suitable for an ECM [13]. Electrospinning of gelatin nanofibers is very versatile so additives (such as polysaccharides) can be easily incorporated with gelatin to overcome the mechanical

inadequacies [14]. Overall, gelatin presents itself as a promising main polymer for an ECM mimic.

Gelatin comes mainly from two main sources: porcine and calf skin. Recently, an increased attention has been paid to gelatin from fish skin (FSG) [5,6]. Utilizing FSG has several benefits to calf skin gelatin as several studies have placed warning that Bovine Spongiform Encephalopathy (BSE) might be transmittable to the host from calf based gelatin [11,12,15]. In addition, FSG is more ethically kosher [5,6] meaning a larger population will be willing to have a transplant surgery with an FSG ECM mimic. Alternatively to calf skin and porcine, FSG can be dissolved in and electrospun from a pure aqueous solution [11]. These qualities make FSG attractive for lowering costs, disbanding with harsh solvents, simplifying syntheses of complex materials, and more creating ethically kosher materials.

Previous studies have demonstrated the syntheses of sustainable ECMs made from gelatin nanofibers and films [16]. This was done by targeting the tissue's ECM morphological properties. The main ECM properties are a random fiber morphology with fiber diameters ranging from 50 to 500 nm [17], a porous structure to allow cell migration [18], and a controlled degradation rate to prevent cells from degrading with the ECM [10]. All these factors point to utilizing electrospun and crosslinked gelatin nanofibrous materials. An advantage of the electrospun method is its natural ability to make a nanofibrous ECM mimic from nanofibers [16]. Further, the degradation rate can be controlled through different methods of crosslinking, e.g., thermal crosslinking, ensuring they are environmentally safe [13].

Some current methods utilized to make gelatin nanofibers can produce the fiber diameter, scaffold porosity, and morphology requirements with a con of a non-aqueous solvent. However, a "green" method suitable for scale-up production has not been fully achieved. One of the current

methods used for gelatin nanofiber construction is centrifugal spinning (C-Spin). C-Spin's main attraction is its simplistic set up to produce fibers [19]. However, ECMs produced by C-Spin have shown poor cell migration into the scaffold [20]. This is due to a large range of fiber diameters on the micro to nanoscales, as two papers indicated gelatin nanofiber diameters ranging from 265 to 632 nm [19–21] which is within the necessary diameter range for the ECM, but are non-uniform [17] further resulting in a low porous scaffold [20]. This method is usually combined with another method (i.e. electrospinning) to overcome these barriers [19,22] taking away from the simplistic set up. As C-Spin usually needs another method to create a good ECM mimic and there are no published flow rates for C-spinning, utilizing alternative synthesis methods for gelatin ECMs is desirable.

Another current method to construct gelatin nanofibers is solution blow spinning (SBS) also referred to as airbrushing [23]. The benefits of SBS is its inexpensive set up and the ability to make versatile fiber compositions [24]. Gelatin fibers have been spun at a flow rate of up to ~1.2 g/h (while others have reported a rate of 1.2 to 2 g/h with SBS) [25,26]. The fiber diameters were as small as 67.5–98.3 nm meeting the tissue's ECM fiber diameter requirement. As seen by the fiber diameter size and good pore size, SBS ECM mimic allows good cell proliferation [23]. Even with this strong benefit of SBS, utilizing another method with a higher production rate would be beneficial for industrial level production.

An alternative method for gelatin fiber construction is Direct Current (DC) electrospinning. Gelatin nanofiber diameters as small as 48 nm have been made with DC electrospinning [27]. The fiber diameter produced by DC electrospinning is uniform providing a suitable surface area to pore size ratio allowing cells to proliferate across the ECM mimic [28,29]. DC electrospinning has a natural ability to construct an ECM mimic [13]. However, a

single capillary DC flow rate is slow averaging at 35–81.6 mg/h [27,30,31]. A milestone of "green" electrospinning was when DC electrospinning spun fish gelatin fibers for the first time from a purely aqueous solution [11]. Even though DC electrospinning can make suitable nanofiber compositions these fibers are electrically charged and must be neutralized before removal causing user risk. While DC electrospinning meets many of the tissue's ECM requirements, this method's production rate is slow and an requires additional neutralization step.

Each of the described methods present benefits and drawbacks from making the ideal ECM. This paper presents a newer method called alternating field electrospinning (AFES) to combine the benefits of the above spinning techniques to construct a better ECM for scale-up production. In this present work, FSG NF's diameters (≤ 300 nm) were successfully prepared at six times higher the rate compared with the current methods. AFES is a high-yield electrospinning technique that has the same advantages as DC electrospinning which are: large surface area to pore size ratio, small nanofiber diameter, and easily varied fiber composition with the additional benefits dense nanofiber flow with no electric charge, high production rate, scale-up production, easy fiber collection, and NF collection without a grounded collector [32–34]. This makes AFES a less expensive and more flexible method to construct a FSG nanofibrous ECM mimic. The ability of AFES to electrospinning porcine and calf skin gelatin has been demonstrated, however, no properties of the scaffolds were tested [35]. Therefore, utilizing AFES to electrospin FSG for an ECM would combine the benefits of both the method and polymer as a viable ECM mimic.

The goal of this study was to develop a "green" AFES method to fabricate a FSG ECM mimic for scale-up production. To keep this method environmentally friendly, in addition to the AFES spinning of FSG NFs from a purely aqueous solution, the nanofibers were crosslinked with no chemicals. AFES was successfully applied at a production rate of 12.6 g/h making FSG

nanofibers with an average narrow and uniform, crosslinked NF diameter range of 100–200 nm. Characterization of cellular response to the fabricated ECM was *in-vitro* tested using naturally fluorescent tdTomato mice fibroblasts that allowed live imaging. These naturally fluorescing cells eliminated an extra dying step and avoided subjecting the scaffold to chemicals that can cause morphology changes in the scaffold making cells pop out of the ECM. This study's results on "green" FSG ECM mimic made by using AFES are presented below.

2. MATERIALS AND METHODS

2.1. Precursor Preparation:

The initial precursors of the biomaterial were made using gelatin from cold water fish skin (Sigma-Aldrich, viscosity 7.0-10.0 CS and pH 4.0-7.5 in 10 wt% solution at 30 °C). Four different FSG precursors were made with 31 wt% FSG in 85–100 wt% of deionized water (dH₂O) solvent with the remainder being acetic acid (AA) (Alfa Aesar, glacial, 99+%). The precursors were then stirred with a Thermix Stirrer (Fisher Scientific, Model 220T) at room temperature. Three more precursors were made with (0, 0.5, 1 wt%) Carboxymethyl cellulose sodium salt (cmCEL) (Scientific Polymer Products, viscosity 1—20 cp at 2 wt% H₂O) with 85–100 wt% dH₂O solvent and the remainder being AA. The more cmCEL contained in the precursor the higher the amount of AA that was required for the cmCEL to be fully dissolved. After fully mixing, FSG 31 wt% was added and stirred with the Thermix Stirrer at room temperature until fully dissolved. All the precursors were AFES spinnable for a period of at least one month after preparation.

2.2. Electrospun Nanofibrous Scaffolds

In a typical process of AFES 30 ml of precursor, Figure 1a, is placed into an automated syringe pump that delivers the precursor to a flat electrode with a 25 mm diameter, Figure 1biiiiv. An AC voltage of 26–39 kV rms voltage is applied to the electrode causing nanofibers to be produced up to 12.6 g/h. The nanofiber flow was driven by electric wind phenomena as a cylindrical mesh shape indicating continuity of long nanofibers, Fig 1bii The nanofibers are collected on a rotating plastic cylinder with a diameter of 10cm, Fig 1bi Nanofibers were produced until a nanofibrous layer thickness reached approximately 200 µm taking 15–30 min depending on the precursor. The nanofiber layer was easily removed from the collector to form a sheet, Fig 1c These nanofibrous sheets (20×25 cm) were then dried in a vacuum chamber for 24 h at room temperature.

2.3. Crosslinking and UV Sterilization

The dried NF sheets were next crosslinked to prevent dissolution in an aqueous solution. The chosen crosslinking method was thermal crosslinking with a temperature ranged from 160 °C to 180 °C in an Isotemp Programmable Muffle Furnace from Fisher Scientific. To choose the prime crosslinking time and temperature, a degradation experiment was performed on the sample FSG, FSGAA-5, and FSG/CEL-5. The nanofiber sheets were crosslinked at two different temperatures and time periods to find this optimal crosslinking procedure: 160°C for four hours, 160°C for eight hours, and 180°C for four hours. For each temperature three samples of FSG, FSGAA-5, and FSG/CEL-5 were used. After crosslinking, the mass and density of each sample were determined. The samples were then immersed in Dulbecco's phosphate buffer saline solution with Ca and Mg (DPBS) (Mediatech) for two time periods, one day and 7 days, in a CO₂ incubator (Lab-Line) at 37°C (normal body temperature). The samples were rinsed in dH₂O and

left to fully dry at room temperature. Once dried, the samples were reweighed to determine the mass retention.

After finding the optimized crosslinking time and temperature based on which samples had the most mass retention, the samples from Table 1 and 2 were crosslinked at the optimized thermal crosslinking procedure of 160°C for eight hours in an Isotemp Programmable Muffle Furnace 650 (Fisher Scientific). Afterward, the NF sheets were cut into discs and placed in a 24 well plate. The samples were briefly exposed to UV light for 10 minutes for sterilization. To determine the effects of thermal and UV treatment, infrared spectroscopy (IR) was performed on these nanofibrous matrices after each stage (before crosslinking, after crosslinking, and after UV sterilization) by using a Fourier Transform Infrared (FTIR) Vertex 70 FTIR spectrometer (Bruker Optics) in transmission mode at a resolution of 2 cm⁻¹ and an average of 32 scans per sample.

2.5. SEM Analysis of Nanofibers

The nanofiber samples were imaged after each of the three stages of fabrication using the scanning electron microscopy (SEM, field-emission scanning electron microscope FEI Quanta 650 FE-SEM), to observe the changes in the matrix's microarchitecture and fibers' morphology. Before SEM imaging, the samples were sputter-coated with a layer of AuPd. After sputter coating to reduce the samples electric charge, the samples were placed in the SEM chamber with a base pressure of 1×10⁻⁴ Pa. SEM images were taken in secondary electron mode with an accelerating voltage of 15 kV, the electron probe current set at 2.5 μA. ImageJ image processing software was then used on the SEM images to determine the nanofiber diameters in each sample before and after crosslinking. A histogram of the nanofiber diameters distribution was constructed for each set of samples.

2.6. Tensile Testing

Preliminary analysis of elastic properties of nanofibrous FSG sheets were carried out using ADMET eXpert 4000 micro tester. The device was equipped with a 5N load cell, MTESTQuattro controller and software. The samples were placed in the custom-made bath and fixed using microclamps with the gauge length set as 10 mm to achieve up to 250 % strain. The sample widths were between 2 and 5 mm. All tests were performed in the custom-made bath in SBF at 37 °C and repeated at least 3 times for each material.

2.7. *In-Vitro* Testing

In-vitro testing was performed on the FSG scaffolds with tdTomato Mice Fibroblasts. Cell media (containing 40,000 cells) was pipetted onto each sample in the well plate. Then the samples (thickness of 200 μm) were placed in an incubator and kept at 37°C. They were checked for cell growth after 24 h, but no noted cell growth was observed on the FSG ECM (a few cells per mm²). There was still relatively little cell growth observed after the 48 h time period. However, after 72 h the cell growth significantly expanded, and the scaffolds were imaged with a microscope (Nikon Eclipse TE-2000U). A few samples were lost during aspiration. Afterwards, Invitrogen-ProLong Diamond Antifade Mountant with DAPI (Thermo Scientific Fisher) was used to stain the tdTomato mice fibroblast's nuclei (as the rest of the cell naturally prefluoresces) and fix the cells. The samples were then mounted onto microscope slides.

The mounted samples' cell growth was viewed with a microscope (Nikon Eclipse TE-2000U), Figure 7. The program Nixon was used to take fluorescent images of the cell growth. Each sample had two images taken of the front and back of the sample. Afterwards, the software ImageJ was used to determine the confluence of the cells, Figure 8a-b. The region statistics of the sample's two pictures were averaged to obtain a uniform distribution on each sample. ImageJ

was again used to identify the number of cells/mm² on the samples. The two pictures of each sample were again averaged together for a uniform number of cell nuclei on each sample, Fig 8a.

2.8. Fluorescing Live Cells

In-vitro testing was again performed on the FSG scaffolds (thickness of 400 μm) with tdTomato Mice Fibroblasts. Cell media (containing 200,000 cells) was pipetted onto each sample in the well plate. More cells and thicker scaffolds were used to gain a more uniform cell proliferation on scaffolds. Then the samples were placed in an incubator and kept at 37°C. After 72 h, cell growth was observed with a microscope (Nikon Eclipse TE-2000U). The scaffolds were removed from the incubator after 72 h of cell growth, and placed in new cell media. Two drops of NucBlue (ThermoFisher Scientific) was added to each well per milliliter of cell media. After 20 min of incubation at room temperature, these scaffolds were imaged live with the Nikon Eclipse TE-2000U microscope.

2.9. Fixing cells

In-vitro testing was performed on the FSG scaffolds (thickness of 200 μm) with tdTomato Mice Fibroblasts. Cell media (containing 190,000 cells) was pipetted onto each sample in the well plate. Higher cell platting was done to ensure large cell growth after 48 h. Then the samples were placed in an incubator and kept at 37 °C. After 48 h, cell growth was observed with a microscope (Nikon Eclipse TE-2000U). The samples then underwent cytoskeleton staining. The scaffolds were rinsed in PBS to remove the cell media. Next, they were fixed with 3.7% methanol-free formaldehyde. The scaffolds were rinsed again with PBS and then permeabilized with 0.1% Triton X-100 in PBS. The scaffolds were again rinsed in PBS. To stain the cell's cytoskeleton two drops of ActinGreentm 488 Ready Probes® Reagent was added to the cell's media per milliliter of media. After 30 min of incubation at room temperature the ActinGreen

solution was removed, and the scaffolds rinsed in PBS again. The scaffolds were then mounted on slides and imaged with the Nikon Eclipse TE-2000U microscope. ImageJ was then used to determine the cell area for each scaffold.

3. Results and Discussion

3.1. Precursor electrospinning and nanofiber production rate

AFES was easily used to electrospin the aqueous precursors listed in Table 1 at a high production rate up to 12.6 g/h. The fully aqueous FSG precursor had the highest flow rate of 36 mL/h. The production rate of AFES was 200 times higher than that reported for DC electrospinning [11]. There was no difference in the flow behavior or nanofiber diameter when changing the electrode size (from 6 to 37.5 mm diameter) or using more than one electrode to increase the productivity. All the precursors in Table 1 exhibited a healthy flow of nanofibers seen in Figure 1b. These nanofibrous flows have a continuous funnel shape while being electrospun. This continuous shape is indicative of long continuous nanofibers. These nanofibers collected onto the cylinder (100–200 rpm, Figure 1bi.) were easily removed from the collector as the final product of AFES nanofibers are uncharged. This is due to the virtual counter electrode created during AFES [36]. The final weight of the FSG nanofiber sheet was 12.6 g after one hour of spinning. This high production rate, ease of machine use, and versatile solution spinning showed that AFES was a good technique to make gelatin nanofibers.

3.2. Thermal Crosslinking

As FSG NFs are completely soluble in an aqueous solution controlling their degradation rate is important for their insertion into a biological environment. Crosslinking has been shown to control nanofibers dissolution rate in an aqueous environment [37]. Thermal crosslinking was

chosen because it is environmentally friendly and cost efficient. The only byproduct of thermal crosslinking gelatin NFs is H₂O [38] and no other costly chemicals are needed to crosslink these fibers. As the only byproduct was water, the nanofibers, Figure 1d-e., showed no visible discoloration or stretching/ tearing after removal from the furnace. This indicated no macro-scale morphological changes due to thermal crosslinking. On a micro-scale, seen in the SEM images in Figure 2a-b., the porosity of the FSG nanofiber sheets decreases as the pores with predominantly triangular shapes shrink a little. This has advantages and disadvantages. A cell needs a certain pore size to proliferate through. If the pore size is too small the cell will not proliferate, and if the pore size is too large the cell will be unable to stay in the ECM due to a bad surface to pore ratio. Finding the optimal crosslinking type and time exposure was necessary for these FSG nanofibers to have this optimal pore size to surface area ratio.

3.3. Nanofiber Diameter

Uniformity of the nanofibers in the nanofibrous sheets is important to provide the cells with consistent nutrients to ingest the nanofibers and proliferate across the sheets. To verify the uniformity of the nanofiber sheet, the non-crosslinked nanofiber diameter measurements were plotted as a histogram, Figure 2a. and then the thermally crosslinked nanofibers at 160° for 8 hours were plotted as a histogram, Figure 2b. The thermally crosslinked nanofiber means with their standard deviations were FSGAA-10 at 175±31 nm, 1 FSGAA-5 at 150±21 nm, FSG/CEL-5 at 175±19 nm, and FSG at 175±41 nm. These nanofibers showed an increase in uniform distribution after thermally crosslinking. This can be seen by the histogram peak being skewed towards the middle. Additionally, all of the nanofiber diameters meet the requirements of the tissues' ECM fiber dimeter range of 50–500 nm [17]. The fiber averages were then compared before and after crosslinking seen in Fig 2b. This graph indicates a decrease in fiber diameter

after crosslinking for FSG, FSGAA-5, and FSG/CEL-5. This is because the main non-harmful byproduct of thermal crosslinking, H₂O, is being removed causing the nanofibers to shrink in diameter [38]. However, the FSGAA-10 showed an increase in fiber diameter when crosslinked. These fibers still showed a loss of H₂O, however, their fiber diameter increase indicated a lateral shrinkage rather than axial. A statistical test, an Anova, was run on the crosslinked nanofiber diameters showing the crosslinked compared to non-crosslinked nanofiber diameters were statistically different. Overall, AFES naturally produces small uniform fiber diameters for the polymer FSG, and thermal crosslinking caused a relatively small axial and lateral fiber shrinkage giving a better fiber uniformity. This provides an even thinner ECM which is necessary for some of the bodies tissue.

3.4. Density of Nanofiber Sheets

To further validate the uniformity of the nanofibrous (NF) sheets, mass density tests were performed to ensure that the nutrients were distributed evenly across each section of the NF sheet. The nanofiber sheets' FSG, FSGAA-10, FSGAA-5, and FSG/CEL-5 density was plotted as a histogram, Figure 4, for each of the thermal crosslinking temperatures and procedures. These histograms show a normal distribution with the mean of FSGAA-10 at 0.04 mg/cm³, FSG/CEL-5 at 0.02 mg/cm³, FSG at 0.06 mg/cm³, and FSGAA-5 at 0.025 mg/cm³. The SD varied between 10–20 % for each NF sheet sample. Even across the varying thermal crosslinking procedures the nanofibers' density stayed uniform. To verify if the uniformity of the produced material, several NF sheets with 30x150 cm were produced in a test scale-up process. No statistically significant variations in fiber diameter, NF sheet mass density, and pore shapes or sizes were noted for either small or large NF sheets prepared from the same precursors and at same AFES parameters. All the density histogram distributions stayed relatively within the SD of

each other's different crosslinking procedures. The only exception was the pure FSG NF sheet crosslinked at 160 °C for 8 h. The density of the sample within itself was uniform, however, the sheet had a much higher density of mean 0.06 mg/cm³ then the other pure FSG nanofiber sheets crosslinked with varying procedures. A t-test was run to show that the FSG NF sheet crosslinked at 160 °C for 8 h had a statistically significant difference compared to the other two FSG NF sheets crosslinking time and temperatures, Figure 4. This was due to the larger volume shrinkage in this FSG nanofiber sheet. Due to non-Newtonian nature of FSG viscosity [39,40] at this temperature and time a density increase is caused. Overall, the thermal crosslinking procedure can vary the fiber's density, but not uniformity within itself. The small amounts of additives also did not affect the nanofiber sheet's density uniformity. As such, the uniformity of the nanofiber's density is independent of the AFES parameter or the size of the produced NF sheet, crosslinking time and temperature and small variations in nanofiber composition, but dependent on the main polymer and solvent.

3.5. Confirming the ECM Structure

As mentioned previously, cells need a good surface area to pore ratio to grow and proliferate across [41]. This desired surface area structure is seen as the normal tissues' ECM structure [28,42]. All AFES spun NF sheets were imaged using SEM to confirm this random fiber morphology structure of the ECM. The ECM structure of the nanofiber sheets can be seen in Figure 1 or Figures 2. Just as the process of DC electrospinning nanofibers mimics the ECM structure [10,13] so does AFES NF mimic the ECM structure of the natural body. Even after thermal crosslinking the nanofiber sheets the ECM structure remains with a small decrease in pore sizes Fig 2a compared to Fig 2b. When cells are seeded to this nanofibrous ECM structure

they still have a good pore size to surface area ratio to attach to and proliferate across with these novel environmentally friendly FSG NF ECMs constructed at a high production rate.

3.6. Degradation tests

Once the nanofibrous ECM structures are inserted into a biological environment controlling the degradation rate of these structures is vital for proper cellular reproduction. If the ECM degrades to quickly the cells will degrade with the ECM as they haven't been able to establish full growth [10]. If the ECM does not degrade quickly enough this could cause an immunogenic response of the body to attack the ECM. As such the FSG ECM NF sheets underwent degradation tests at the three varying crosslinking times and temperatures. The percentage of mass retained of each of these ECM can be seen in Figure 5. The FSG nanofiber ECM that were thermally crosslinked at 160 °C for 8 h retained the most mass over the 2-week period. As such all nanofibrous ECMs were crosslinked at 160 °C for 8 h for *in-vitro* tests. The other crosslinking procedures would have caused the cells to degrade and be lost with the ECM. Also seen in Figure 5a-5c the addition of cmCEL to the FSG ECM strengthened its integrity further slowing its degradation rate. These degradation tests indicated thermal crosslinking can be used as a "green" method to control fibers degradation rate while the importance cmCEL additives can further slow the degradation rate of the nanofibers.

3.7. Mechanical Behavior of FSG Scaffolds in SBF

The tensile behavior of all scaffolds immersed in SBF at 37 °C demonstrated similar behavior after either 1 day or 3 days exposure. The recorded engineering stress-strain curves exhibited an extended toe region (from 50 to 150 % strain) due to the gradual realignment of nanofibers along the direction of stretching followed by a linear segment. The linear segments were used to determine the Young's moduli (Table 3) that has been shown to affect the cells

viability, proliferation, and spreading. The elongation at break was more than 200 % for all samples, which hindered the determination and comparison of maximum stress due to the limit of the instrument. The Young's moduli of the samples exposed in SBF for 24 h increased in the sequence FSG < FSGAA-5 < FSGAA-10 < FSG-CEL-5. The numbers varied, respectively, from ~5.6 kPa for FSG to 32.8 kPa for FSG-CEL-5, with other materials being between. Most scaffolds still maintained 69–85 % of their maximum moduli after 72 h in SBF, except FSG sample (10–16 %) that degraded faster.

The increase of strength and elastic modulus of polymer nanofibers with the addition of cmCEL has been observed [43, 44]. When compared to the scaffold mass density in Fig.4, it can be noted that FSG-CEL-5 and FSGAA-5 scaffolds have the lowest density. Because the both tensile strength and modulus depend strongly on the density of porous material [45], this means that the individual fibers in FGAA-5 may actually have higher modulus than those in FSGAA-10 scaffold. Those factors can explain a better cell initial attachment and proliferation on FSG-CEL-5 and FSGAA-5 scaffolds. The elastic moduli of the scaffolds are slightly lower than those for the human body ECMs but still give the cells a suitable substrate to grow on.

3.8. FTIR on Nanofiber ECMs

To further validate the uniformity and degradation of the nanofibrous ECMs FTIR was used to confirm any molecular structural changes in the nanofibers. The FITR graphs before thermal crosslinking, Figure 6b indicate no strong differences in the absorption bands other than the cellulose band seen at 1000 cm⁻¹. The molecular structures after thermal crosslinking the scaffolds at 160 °C for 8 h also show no molecular structural changes compared to the non-crosslinked fibers. However, after sterilizing these scaffolds with UV light (which slightly crosslinks) minimal oxidation of the FSG/CEL-5 nanofiber ECM can be seen in the band region

1700 cm⁻¹ Figure 6a. While thermally crosslinking causes no degradation, UV sterilization can cause some molecular degradation. This is not enough degradation to affect the cell growth but utilizing a different sterilization method could improve cell growth by preventing the loss of the cellulose additive. These FTIR graphs show again that using thermal crosslinking compared to other kinds of crosslinking retains the uniformity and molecular structure of the original nanofiber composition.

3.9. Analyzing Cell Growth

The uniform nanofiber scaffolds were confirmed to be a biomaterial with a successful invitro testing of tdTomato fibroblasts. Figures 7a-d shows that the FSGAA-5 scaffold had the largest confluence of cells across it at 14.4%. The main differences in this scaffold were a smaller fiber diameter and a lower density. These two factors provided a better surface area to pore size ratio for the cells to spread across. The pure FSG ECM had the largest number of cells per area (251±179 cells/mm²) and also the largest density per unit area providing a large surface area for cells to seed into, however confluence was lower due to smaller pore size of the denser material. The FSG/CEL-5 ECM had the largest amount of confluence 11.4% with the least cells 198±104 cells/mm², giving this ECM the largest cells. The only variation between the FSG/CEL-5 ECM and FSGAA-5 ECM was the addition of the cellulose. The effect of the cellulose additive in the ECM was very beneficial as it provided more nutrients to the cells that attached allowing them to grow larger and stabilize. This is seen when comparing the FSG/CEL-1 and FSGAA-15 ECMs, Figures 8c and 8f. The only difference was the 1 % cmCEL which increased confluence by 9 % overcoming any side effects caused by the AA with a cell number of 235±80 cells/mm². Overall, these ECMs showed good, healthy cell growth and proliferation. The factor that affected the cell growth the most between the AFES spun nanofiber sheets density, nanofiber diameter,

ECM structure, surface to area ratio (pores size), the composition (molecular structure), and pore sites. The composition of the nanofiber was the strongest factor of affecting cell growth as seen between the FSGAA-15 and FSG/CEL-1 ECMs. Additionally, increased amounts of cmCEL decreased the SD of the cell number in the ECM causing more uniformity. However, increasing the surface area to pore size ratio of these FSG/CEL nanofiber dimeters (to the FSG fibers density) might further provide more sits for cells to attach and proliferate across the ECM.

3.10. GFP fluorescing compared to tdTomato

The tdTomato mice fibroblasts are a novel way to observe cell proliferation across a scaffold. Their use for live imaging of cells is becoming more prevalent since their first use in 2004 [43]. To compare tdTomatoes natural fluorescence of the cell's mitochondria to a well-known staining of the cell's actin with the green fluorescent protein (GFP) the area of the same fibroblasts on the FSG ECM, fluoresced at 620 nm and 570 nm, were compared. A T-test was performed and showed that the tdTomato and GFP fluorescence were not statistically significantly different. This shows that either method can be used for staining cells to obtaining cell area [44]. Utilizing both stains together can give a better overall cells morphology as seen in Fig. 9ai and 9bi. However, the formaldehyde used in the GFP staining can cause the cells to shrivel and change the cell's morphology from its natural morphology in a biological environment. The additional step of dying the cells on the FSG ECM could potentially be avoided further lowering cost and saving time. As seen in Fig.8b the uniqueness of these tdTomato cells additionally allows for live imaging as the cells might not always need to be fixed as in the use of GFP.

3.11. Live Cell Imaging

Live Imaging of the tdTomato mice fibroblasts on the FSG ECM was achieved as tdTomato naturally fluoresces [46,47]. Viewing these cells live gives a better image of how the cells interact in their biological environment on the FSG ECM Fig.8b and allows additional information to be obtained from the cells that is lost by harsh chemicals during dying [47,48]. Comparing the live tdTomato fibroblasts (Fig.8b) to the fixed cells (Fig.8a) the live cells are seen to be more elongated as the imaging was done dynamically rather than statically. Additionally, Fig.8b only shows one layer of the FSG ECM. The fixed cells in figure 8a are slightly out of proportion as they were mounted to a microscope slide and flattened. Flattening the FSG ECM allowed more visibility of cells through the ECM, which is a beneficial but viewing an uncompressed FSG ECM depicts a better image of the cells in their natural biological environment and also eliminates an additional step and cost of mounting slides.

4. Conclusion

A low-cost, "green" fabrication of fish skin gelatin (FSG) nanofibrous extracellular matrix (ECM) was achieved at a high productivity rate by using alternating field electrospinning (AFES) and thermal crosslinking of an as-spun product. A production rate of 12.6 g/h of nanofibrous ECM material has been achieved, which significantly exceeds the reported values for different spinning methods and still can be scaled up easily. The AFES method produced FSG ECMs that have fiber diameters in a 100–200 nm range with a narrow size distribution and good pore to surface ratio to provide a desired scaffold for cells to proliferate across. Thermal crosslinking has been shown to not cause any nanofiber morphology changes or deformation of the ECM while providing controlled degradation rates of the ECMs. The performance of AFES

produced FSG ECMs is very sensitive to the changes in the composition of precursor solution. It has been shown that small modifications of the solvent (e.g., acetic acid addition) or polymer (e.g., carboxymethyl cellulose addition) strongly affect the density, degradation rates and cellular response of the fabricated ECMs without significant changes in fiber diameter and surface morphology. Overall, AFES fabricated FSG ECM shows promising results for a base biomaterial that is bioactive, biocompatible, and suitable for scale-up manufacturing.

Acknowledgements

A.K. and M.A. were supported through the NSF-IRES awards (Grant #1558268 and #1852207)

Competing Interest Statement

There are no financial or personal conflicts of interest.

REFERENCES:

- [1] Gao X, Han S, Zhang R, Liu G, Wu J. Progress in electrospun composite nanofibers: composition, performance and applications for tissue engineering. J Mater Chem B. 2019;7(45):7075–89.
- [2] Frantz C, Stewart KM, Weaver VM. The extracellular matrix at a glance. J Cell Sci. 2010;123(24):4195–200.
- [3] Ghassemi Z, Slaughter G. Storage stability of electrospun pure gelatin stabilized with EDC/Sulfo-NHS. Biopolymers. 2018;109(9):e23232.
- [4] Silva KD, Kumar P, Choonara YE, Toit LC du, Pillay V. Three-dimensional printing of extracellular matrix (ECM)-mimicking scaffolds: A critical review of the current ECM materials.

 J Biomed Mater Res A. 2020;108(12):2324–50.

- [5] Huang T, Tu Z, Shangguan X, Sha X, Wang H, Zhang L, et al. Fish gelatin modifications: A comprehensive review. Trends Food Sci Technol. 2019;86:260–9.
- [6] Karim AA, Bhat R. Fish gelatin: properties, challenges, and prospects as an alternative to mammalian gelatins. Food Hydrocoll. 2009;23(3):563–76.
- [7] Lee KY, Mooney DJ. Hydrogels for Tissue Engineering. Chem Rev. 2001;101(7):1869–80.
- [8] Ponticos M, Partridge T, Black CM, Abraham DJ, Bou-Gharios G. Regulation of Collagen Type I in Vascular Smooth Muscle Cells by Competition between Nkx2.5 and δEF1/ZEB1. Mol Cell Biol. 2004;24(14):6151–61.
- [9] Ghassemi Z, Slaughter G. Cross-linked electrospun gelatin nanofibers for cell-based assays. Conf Proc Annu Int Conf IEEE Eng Med Biol Soc IEEE Eng Med Biol Soc Annu Conf. 2018;2018:6088–91.
- [10] Gomes SR, Rodrigues G, Martins GG, Roberto MA, Mafra M, Henriques CMR, et al. In vitro and in vivo evaluation of electrospun nanofibers of PCL, chitosan and gelatin: A comparative study. Mater Sci Eng C. 2015;46:348–58.
- [11] Kwak HW, Shin M, Lee JY, Yun H, Song DW, Yang Y, et al. Fabrication of an ultrafine fish gelatin nanofibrous web from an aqueous solution by electrospinning. Int J Biol Macromol. 2017;102:1092–103.
- [12] Gomes SR, Rodrigues G, Martins GG, Henriques CMR, Silva JC. In vitro evaluation of crosslinked electrospun fish gelatin scaffolds. Mater Sci Eng C. 2013;33(3):1219–27.
- [13] Campiglio CE, Contessi Negrini N, Farè S, Draghi L. Cross-Linking Strategies for Electrospun Gelatin Scaffolds. Materials. 2019;12(15):2476.
- [14] Hickey RJ, Pelling AE. Cellulose Biomaterials for Tissue Engineering. Front Bioeng Biotechnol Front Bioeng Biotechnol. 2019; 7: 45. 15.

- [15] Gómez-Guillén MC, Pérez-Mateos M, Gómez-Estaca J, López-Caballero E, Giménez B, Montero P. Fish gelatin: a renewable material for developing active biodegradable films. Trends Food Sci Technol. 2009;20(1):3–16.
- [16] Xie X, Chen Y, Wang X, Xu X, Shen Y, Khan A ur R, et al. Electrospinning nanofiber scaffolds for soft and hard tissue regeneration. J Mater Sci Technol. 2020;59:243–61.
- [17] Smith IO, Liu XH, Smith LA, Ma PX. Nanostructured polymer scaffolds for tissue engineering and regenerative medicine. WIREs Nanomedicine Nanobiotechnology. 2009;1(2):226–36.
- [18] Murphy CM, Haugh MG, O'Brien FJ. The effect of mean pore size on cell attachment, proliferation and migration in collagen–glycosaminoglycan scaffolds for bone tissue engineering. Biomaterials. 2010;31(3):461–6.
- [19] Loordhuswamy AM, Krishnaswamy VR, Korrapati PS, Thinakaran S, Rengaswami GDV. Fabrication of highly aligned fibrous scaffolds for tissue regeneration by centrifugal spinning technology. Mater Sci Eng C. 2014;42:799–807.
- [20] Haider A, Haider S, Rao Kummara M, Kamal T, Alghyamah A-AA, Jan Iftikhar F, et al. Advances in the scaffolds fabrication techniques using biocompatible polymers and their biomedical application: A technical and statistical review. J Saudi Chem Soc. 2020;24(2):186–215.
- [21] Xia L, Lu L, Liang Y, Cheng B. Fabrication of centrifugally spun prepared poly(lactic acid)/gelatin/ciprofloxacin nanofibers for antimicrobial wound dressing. RSC Adv. 2019;9(61):35328–35.

- [22] Jana H, Tomáš S, Monika Š, Marek P, Koš K. A comparison of the centrifugal force spinning and electrospinning of collagen under different conditions. Proc. 8th Int. Conf. Nanomater. Res. Appl. 2016; 514–519.23.
- [23] Daristotle JL, Behrens AM, Sandler AD, Kofinas P. A Review of the Fundamental Principles and Applications of Solution Blow Spinning. ACS Appl Mater Interfaces. 2016;8(51):34951–63.
- [24] Medeiros ES, Glenn GM, Klamczynski AP, Orts WJ, Mattoso LHC. Solution blow spinning: A new method to produce micro- and nanofibers from polymer solutions. J Appl Polym Sci. 2009;113(4):2322–30
- [25] Liu F, Türker Saricaoglu F, Avena-Bustillos RJ, Bridges DF, Takeoka GR, Wu VCH, et al. Preparation of Fish Skin Gelatin-Based Nanofibers Incorporating Cinnamaldehyde by Solution Blow Spinning. Int J Mol Sci. 2018 Feb 22;19(2):618
- [26] Vilches JL, Souza Filho M de SM de, Rosa M de F, Sanches AO, Malmonge JA, Vilches JL, et al. Fabrication of Fish Gelatin Microfibrous Mats by Solution Blow Spinning. Materials Research. 2019; 22(suppl. 1): e20190158
- [27] Beishenaliev A, Lim SS, Tshai KY, Khiew PS, Moh'd Sghayyar HN, Loh H-S. Fabrication and preliminary in vitro evaluation of ultraviolet-crosslinked electrospun fish scale gelatin nanofibrous scaffolds. J Mater Sci Mater Med. 2019;30(6):62.
- [28] Nemati S, Kim S, Shin YM, Shin H. Current progress in application of polymeric nanofibers to tissue engineering. Nano Converg 2019; 6: 36 29.
- [29] Courtenay JC, Sharma RI, Scott JL. Recent Advances in Modified Cellulose for Tissue Culture Applications. Molecules. 2018;23(3):654.

- [30] Barati F, Farsani AM, Mahmoudifard M. A promising approach toward efficient isolation of the exosomes by core–shell PCL-gelatin electrospun nanofibers. Bioprocess Biosyst Eng. 2020;43(11):1961–71.
- [31] Pankongadisak P, Tsekoura E, Suwantong O, Uludağ H. Electrospun gelatin matrices with bioactive pDNA polyplexes. Int J Biol Macromol. 2020;149:296–308.
- [32] Lawson C, Stanishevsky A, Sivan M, Pokorny P, Lukáš D. Rapid fabrication of poly(ε-caprolactone) nanofibers using needleless alternating current electrospinning. J Appl Polym Sci 2016;133(13):43232
- [33] Pokorny P, Kostakova E, Sanetrnik F, Mikes P, Chvojka J, Kalous T, et al. Effective AC needleless and collectorless electrospinning for yarn production. Phys Chem Chem Phys. 2014;16(48):26816–22.
- [34] Stanishevsky A, Tchernov J. Mechanical and transport properties of fibrous amorphous silica meshes and membranes fabricated from compressed electrospun precursor fibers. J Non-Cryst Solids. 2019;525.
- [35] Jirkovec R, Kalous T, Brayer WA, Stanishevky AV, Chvojka J. Production of gelatin nanofibrous layers via alternating current electrospinning. Mater Lett. 2019;252:186–90.
- [36] Drews AM, Cademartiri L, Whitesides GM, Bishop KJM. Electric winds driven by time oscillating corona discharges. J Appl Phys. 2013;114(14):143302.
- [37] Kwak HW, Park J, Yun H, Jeon K, Kang D-W. Effect of crosslinkable sugar molecules on the physico-chemical and antioxidant properties of fish gelatin nanofibers. Food Hydrocoll. 2021;111:106259.
- [38] Gomes SR, Rodrigues G, Martins GG, Henriques CMR, Silva JC. In vitro evaluation of crosslinked electrospun fish gelatin scaffolds. Mater Sci Eng C. 2013;33(3):1219–27.

- [39] Chandra MV, Shamasundar BA, Kumar PR. Visco-Elastic and Flow Properties of Gelatin from the Bone of Freshwater Fish (Cirrhinus mrigala). J Food Sci. 2013;78(7):E1009–16.
- [40] Heyns JD, Ahmed Mohamed ET, Declercq NF. Non-linear ultrasonic and viscoelastic properties of gelatine investigated in the temperature range of 30 °C–60 °C. Phys Fluids. 2021;33(2):022002.
- [41] Hu W-W, Yu H-N. Coelectrospinning of chitosan/alginate fibers by dual-jet system for modulating material surfaces. Carbohydr Polym. 2013;95(2):716–27.
- [42] Liguori A, Uranga J, Panzavolta S, Guerrero P, de la Caba K, Focarete ML. Electrospinning of Fish Gelatin Solution Containing Citric Acid: An Environmentally Friendly Approach to Prepare Crosslinked Gelatin Fibers. Materials. 2019;12(17):2808.
- [43] Goudarzi Z M., Behzad, T, Ghasemi-Mobarakeh, L, Kharaziha, M., Enayati, MS, Structural and mechanical properties of fibrous poly (caprolactone)/gelatin nanocomposite incorporated with cellulose nanofibers. Polymer Bulletin. 2020; 77(2):717–40.
- [44] Paulett K, Brayer WA, Hatch K, Kalous T, Sewell J, Liavitskaya T, Vyazovkin S, Liu F, Lukáš D, Stanishevsky A. Effect of nanocrystalline cellulose addition on needleless alternating current electrospinning and properties of nanofibrous polyacrylonitrile meshes. J. Appl. Polym. Sci. 2018; 135 (5); 45772.
- [45] Gibson LJ, Ashby MF, Cellular solids: structure and properties, Second ed., Cambridge University Press, Cambridge, UK, 1997.
- [46] Syverud BC, Gumucio JP, Rodriguez BL, Wroblewski OM, Florida SE, Mendias CL, et al. A Transgenic tdTomato Rat for Cell Migration and Tissue Engineering Applications. Tissue Eng Part C Methods. 2018;24(5):263–71.

- [47] Prusicki MA, Balboni M, Sofroni K, Hamamura Y, Schnittger A. Caught in the Act: Live-Cell Imaging of Plant Meiosis. Front Plant Sci.2021;12.
- [48] Prusicki MA, Balboni M, Sofroni K, Hamamura Y, Schnittger A. Caught in the Act: Live-Cell Imaging if Plant Meiosis. Front Plant Sci. 2021;12.



Figure 1: Process of creating and *in-vitro* testing the FSG biomaterial. (a) The FSG precursor has a consistency of syrup. (b) The AFES process, (iv) electrode that the (iii) FSG precursor is placed on. After creating a potential difference in the FSG precursor (ii) nanofibers are lifted by ionic winds and initial impulse of the created fibers to the (i) collector which rotates collecting sheets of (c) nanofibers. (c.i.) A similar morphology to the ECM can be seen with an SEM image. (d) After confirmation, the nanofibers thermally crosslinked in an oven. After sterilization (e) *in-vitro* seeding of tdTomato fibroblasts confirms that the FSG is a viable biomaterial with (e.i.) cell growth.

2-column fitting image

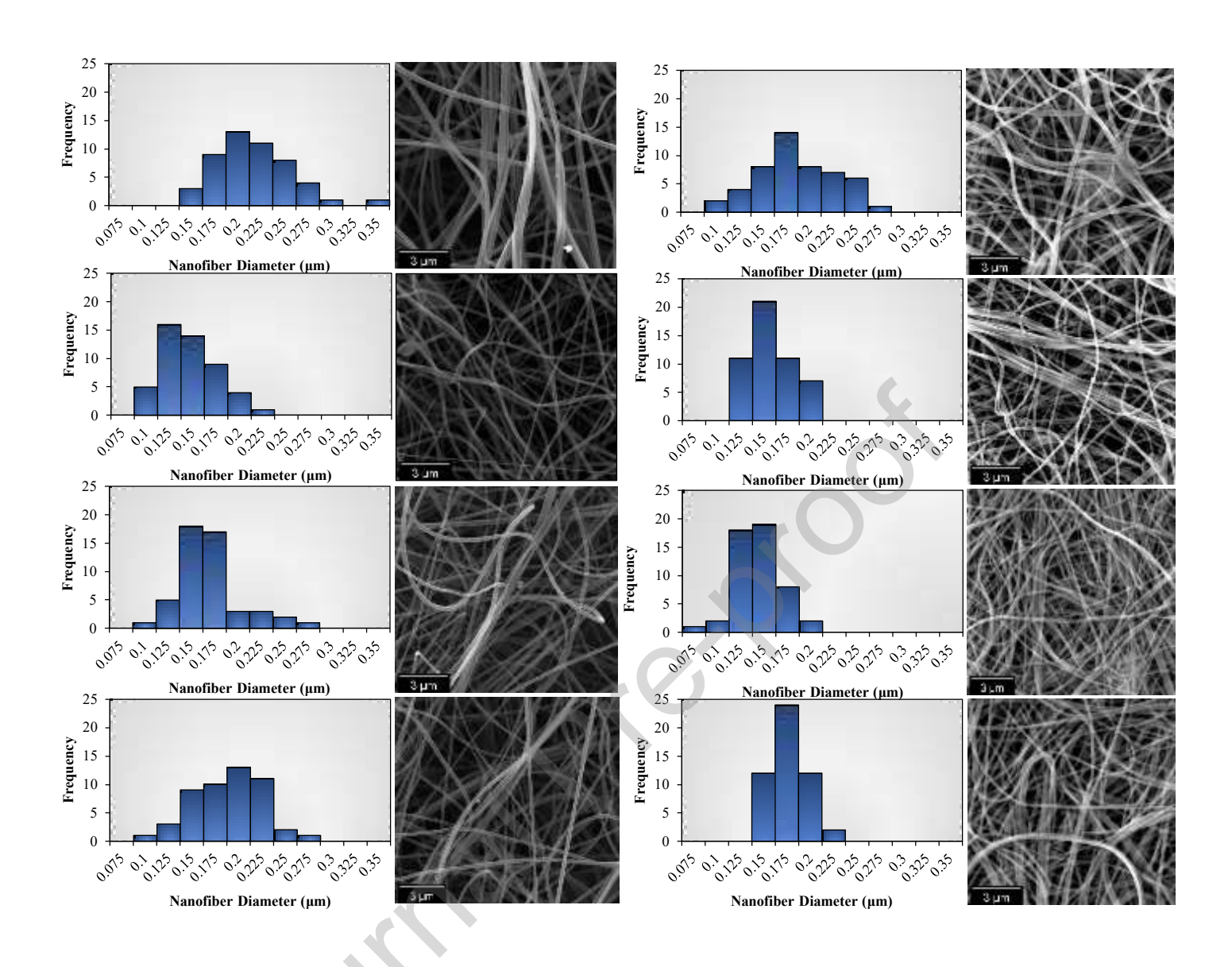


Figure 2: SEM images and distribution of nanofiber diameters before thermal crosslinking and after thermal crosslinking. Before thermal crosslinking are (a) FSG (b) FSGAA-10 (c) FSGAA-5 (d) FSG/CEL-5. Histogram of uniform nanofiber diameters after thermal crosslinking where visible shrinkage in fiber diameter can be observed by the peaks shifting left. A side effect of thermal crosslinking was causing more uniform fiber diameters seen by the peak being skewed to the middle (e) FSG (f) FSGAA-10 (g) FSGAA-5 (h) FSG/CEL-5

2-column fitting image

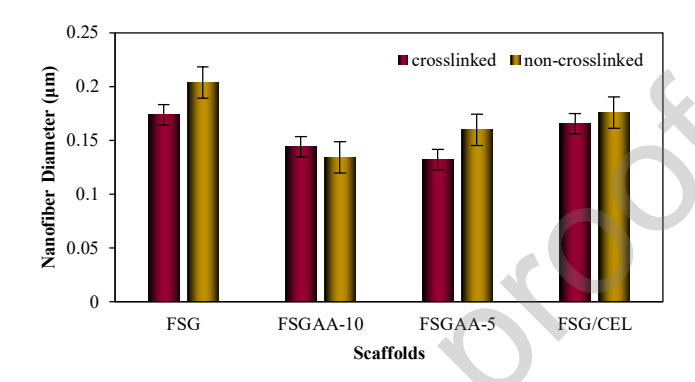


Figure 3: Average fiber diameters of the different scaffolds comparing non-crosslinked to thermally crosslinked scaffolds. FSG, FSGAA-5, FSG/CEL-5 nanofiber diameters all shrank axially, while FSGAA-10 indicated a lateral increase in fiber diameters.

Single column fitting image

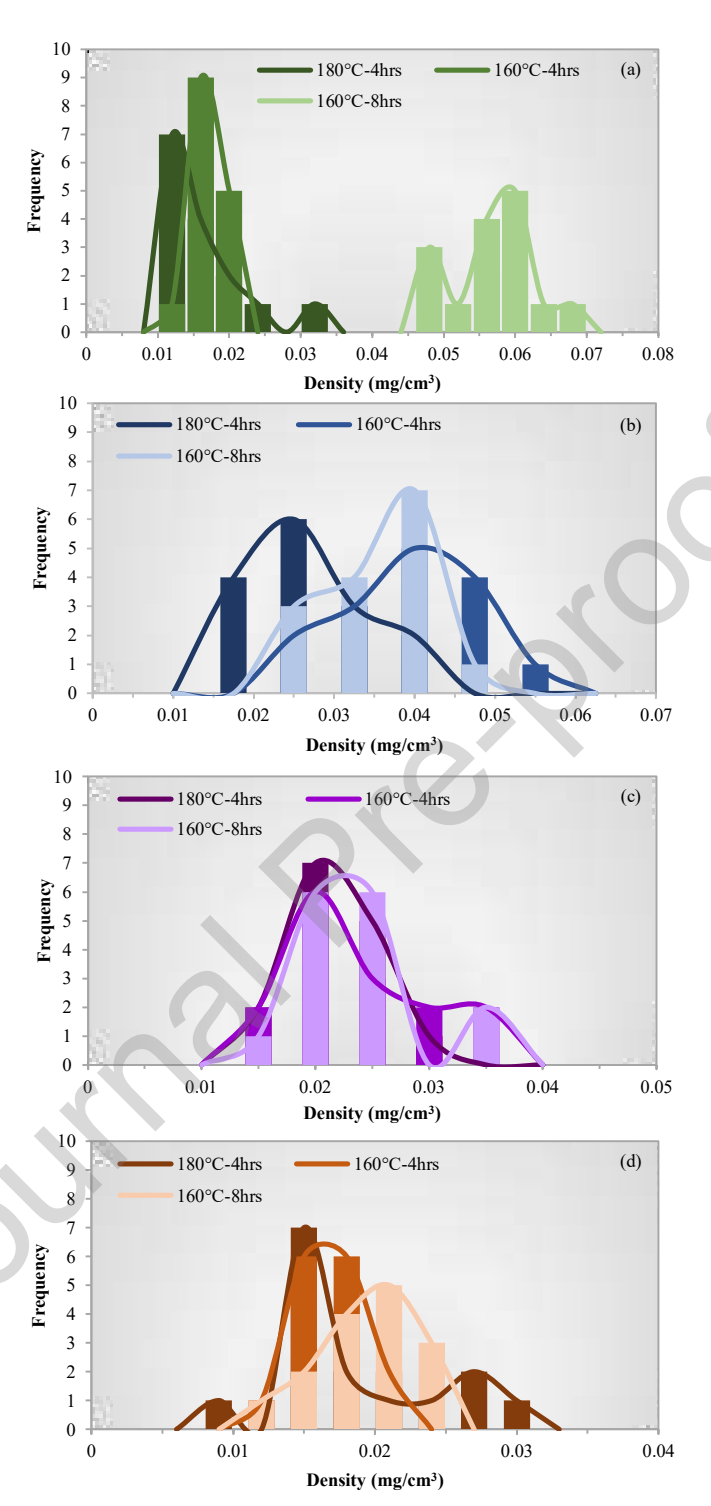
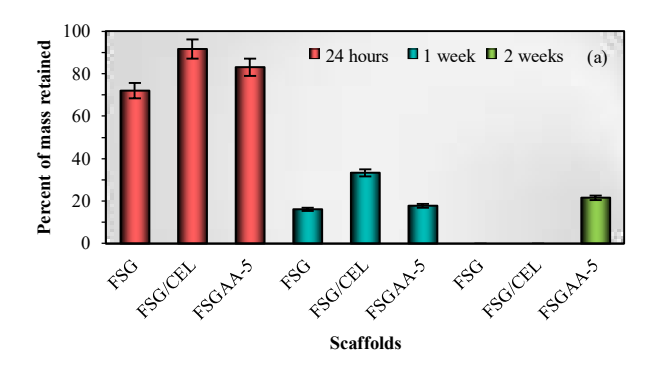
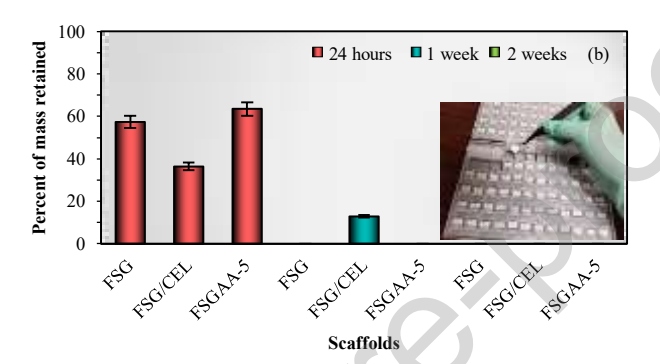


Figure 4: Density histograms of the nanofiber sheets showing a uniform distribution over different cross sections of the sheet. The peak of each histogram normally lies at the same density except for (a) FSG nanofiber which indicate a higher density for crosslinking at 160°C for 8 hours due to FSG non-Newtonian nature. The other nanofiber sheets (b) FSGAA-10 (c) FSGAA-5 and (d) FSG/CEL show a normal distribution for all crosslinking procedures around the same density.





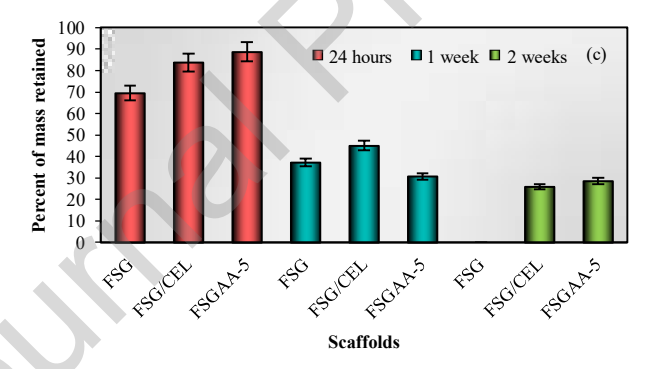
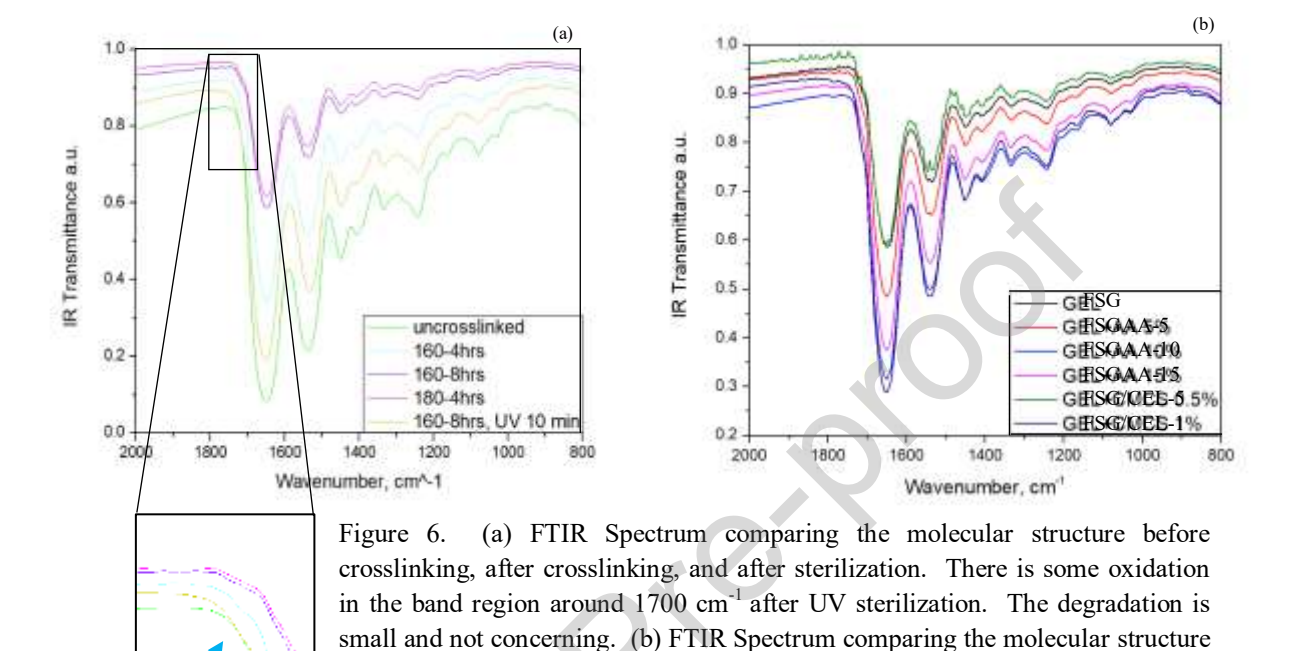


Figure 5: Percent of mass retained of the whole scaffold for varying thermal crosslinking procedures. The nanofiber scaffolds were thermal crosslinked at (a) 180°C for 4 hours (b) 160°C for 4 hours and (c) 160°C for 8 hours. The samples thermally crosslinked at 160°C for 8 hours retained the most mass, and the addition of cmCEL made the nanofiber scaffold retain even more mass then the pure FSG nanofiber scaffold.

Single column fitting image



between the varying nanofiber composition in Table 1 and 2. All spectra show the same trend except FSG/CEL 5 and 10 have a cellulose band in the 1000 cm⁻¹

2-column fitting image

region.

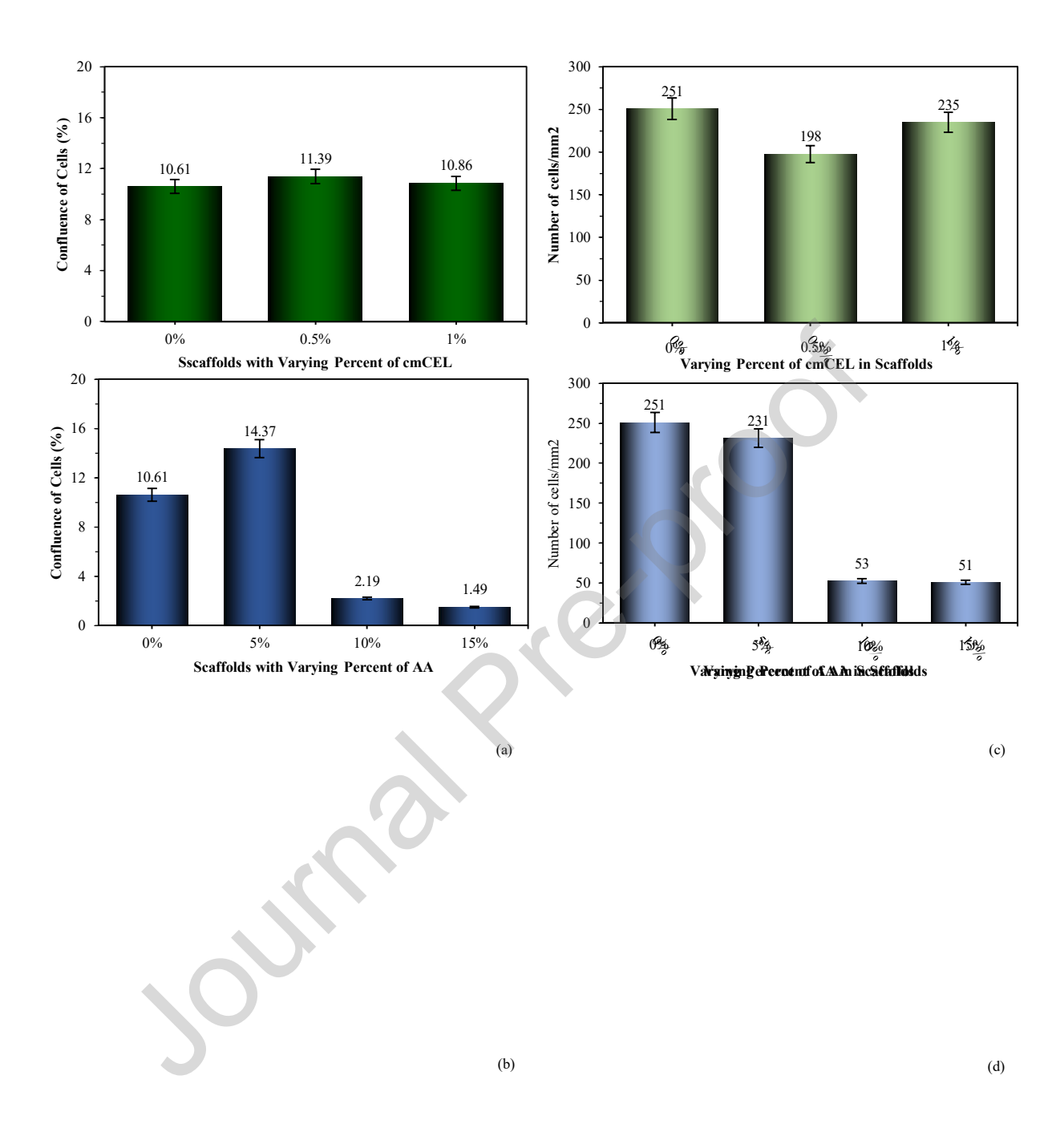


Figure 7: Proliferation and healthy cell growth across the varying scaffolds from Table 1 and 2. (a) The scaffolds with 0.5% cmCEL had the largest confluence. (b) the FSGAA-5 scaffold showed a higher cell confluence. This scaffold held the same nanofibeg somposition as the FSG/CEL-5 without the additional 0.5% cmCEL (c) These 5% cmCEL scaffolds had the largest area of cells (d) compared to the FSGAA-5

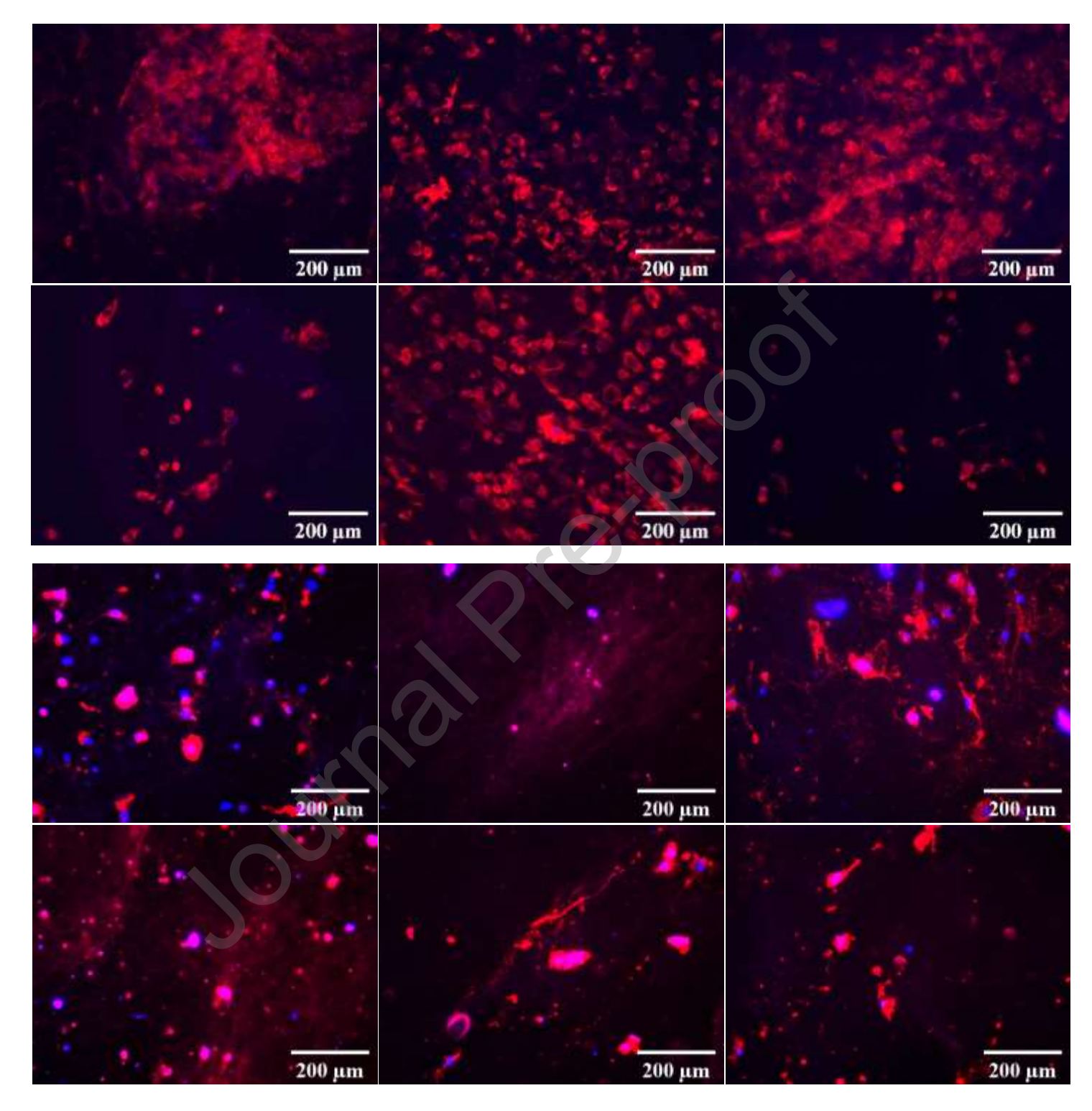


Figure 8: (a) Fluorescence images of fixed tdTomato fibroblasts proliferation across the varying ECM compositions: (a.i.) FSG (a.ii.) FSG/CEL-5 (a.iii.) FSG/CEL-1 (a.iv.) FSGAA-5 (a.v.) FSGAA-10 (a.vi.) FSGAA-15. The difference in the cell proliferation between the ECM with cmCEL compared to those without can strongly be seen between (a.iii.) and (a.vi.). (b) Fluorescence images of live TdTomato fibroblasts proliferation across the varying ECM compositions: (b.i.) FSG (b.ii.) FSG/CEL-5 (b.iii.) FSG/CEL-1 (b.iv.) FSGAA-5 (b.v.) FSGAA-10 (b.vi.) FSGAA-15. The individual nanofiber strands with cells proliferating across the ECM can be seen best in (b.ii.) and (b.iv.)

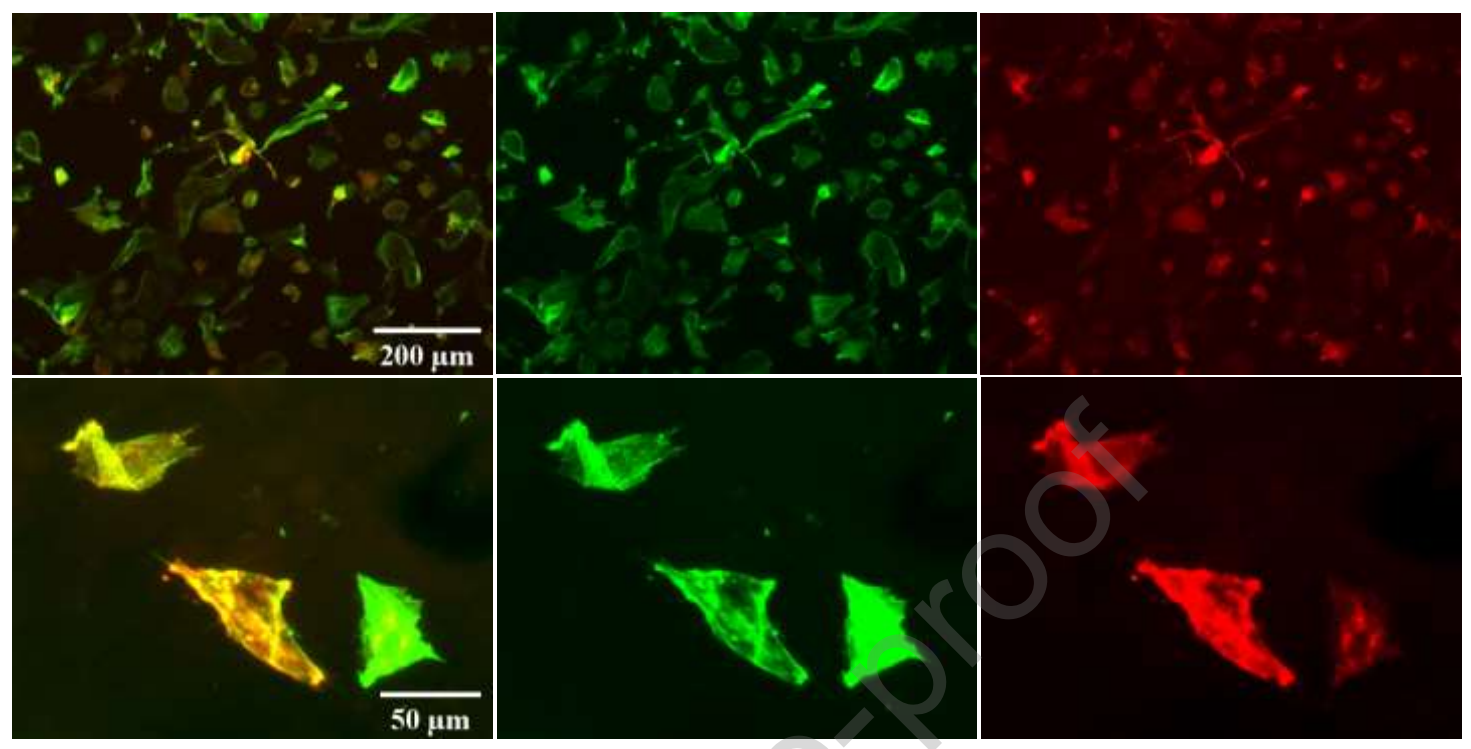


Figure 9: (a) Composite fluorescence image of (i) FSG/Cell-1 ECM in comparison with only(ii) GFP fluorescence and (iii) tdTomato natural fluorescence of the fibroblasts; (b) Composite fluorescence image at ×400 of(i) FSGAA-5 ECM in comparison with only (ii) the GFP fluorescence of the cell's actin and (iii) the tdTomato fluorescence of the mitochondrial

2-column fitting image

Table 1. Precursor compositions for pure FSG nanofiber with varying amounts of AA.

Materials	FSG (wt%)	FSGAA-5 (wt%)	FSGAA-10 (wt%)	FSGAA-15 (wt%)
FSG	31	31	31	31
dH ₂ O	69	65.6	62.1	58.6
AA	-	4	6.9	10.3

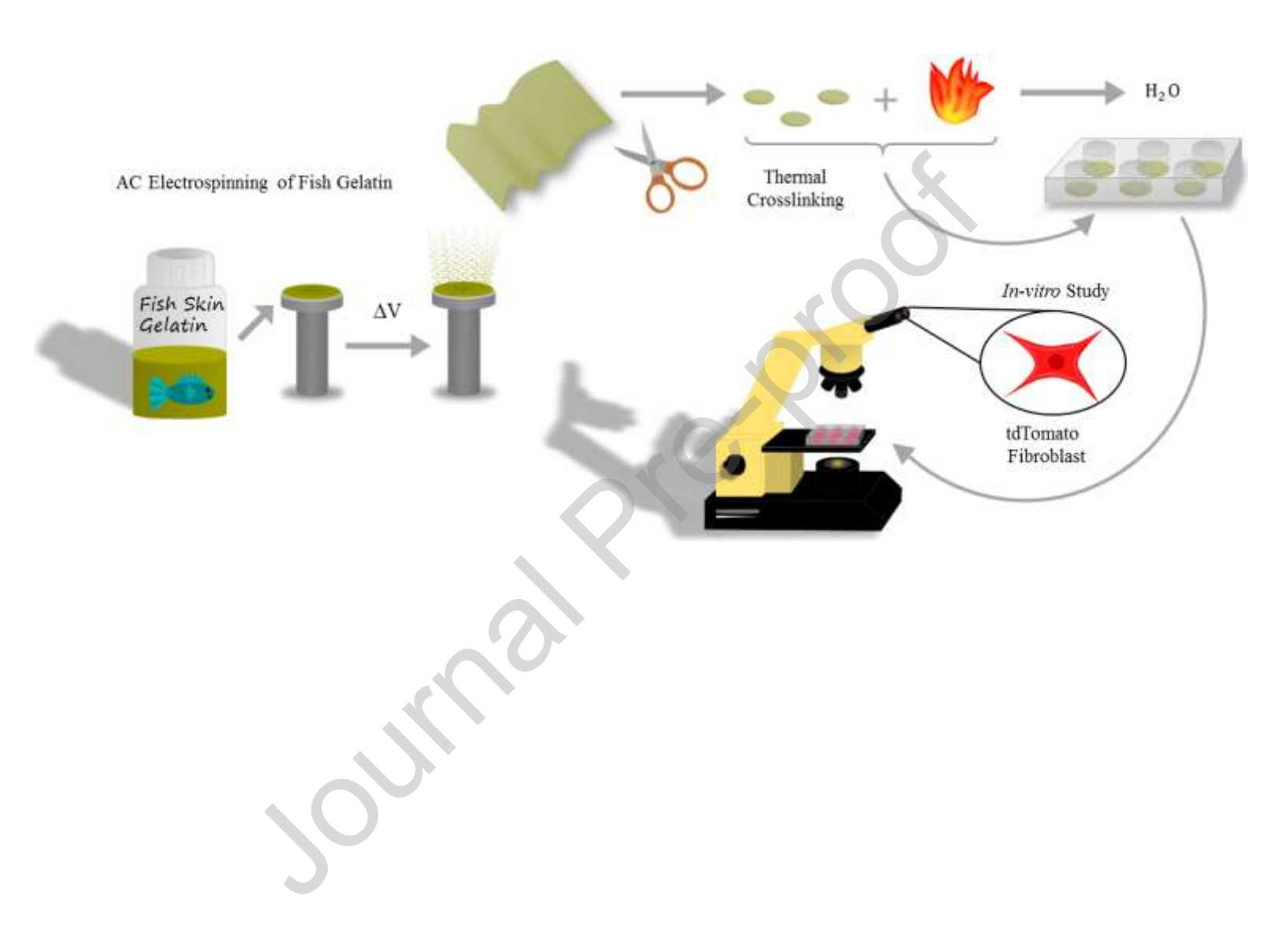
Table 2. Precursor compositions of FSG nanofibers with varying amounts of cmCEL.

Materials	FSG (wt%)	FSG/CEL 5 (wt%)	FSG/CEL 1 (wt%)
Cellulose	-	0.3	.3
FSG	31	31	31
dH ₂ O	69	65.3	58.4
AA	-	3.4	10.3

Table 3. Young's moduli of fish gelatin based nanofibrous scaffolds tested under tensile load after the exposure in SBF for 1 and 3 days.

Exposure		Young's Modulus, kPa			
Time, h	FSG	FSG/CEL-5	FSGAA-5	FSGAA-10	
24 h	5.6±1.4	32.8±3.4	12.1±2.2	21.1±2.9	
72 h	0.52±0.2	23.8±3.1	9.0±1.7	17.7±2.6	

Graphical Abstract



Authors' Contributions

Amanda Kennell—Conceptualization, Methodology, Validation, Formal Analysis, Investigation, Data

Curation, Writing - Original Draft, Writing - Review & Editing, and Project Administration

Mark MacEwen— Methodology, Writing – Review and Editing

Micah Armstrong—Writing – Review and Editing

Nicola Teodora—Methodology and Investigation

Brian Halloran— Methodology and Investigation

Namasivayan Ambalavanan—Conceptualization, Resources, and Writing – Review and Editing Andrei Stanishevsky—Writing-Review & Editing, Conceptualization, Resources, Supervision, and

validation

Declaration of interests

oxtimes The authors declare that they have no known competing financial interests or personal relationships that could have appeared to influence the work reported in this paper.
☐The authors declare the following financial interests/personal relationships which may be considered as potential competing interests:

Highlights

- Environmentally safe, biocompatible, uniform, fish skin gelatin nanofibrous matrix
- Scale-up production method with Alternating Field Electrospinning (AFES)
- High production rate (12.6g/h) of uniform gelatin nanofiber diameters (175±41 nm)
- In vitro tested gelatin Extracellular matrix with tdTomato mice fibroblasts